Inorg. Chem. **2006**, *45*, 83–93

Synthesis, Structure, and Magnetic Behavior of a Series of Trinuclear Schiff Base Complexes of 5f (U^{IV}, Th^{IV}) and 3d (Cu^{II}, Zn^{II}) Ions

Lionel Salmon,*,† Pierre Thuéry,† Eric Rivière,‡ and Michel Ephritikhine*,†

Service de Chimie Moléculaire, DSM, DRECAM, CNRS URA 331, Laboratoire Claude Fréjacques, CEA/Saclay, 91191 Gif-sur-Yvette, France, and Laboratoire de Chimie Inorganique, Institut de Chimie Moléculaire et des Matériaux, CNRS UMR 8613, Université de Paris-Sud, 91405 Orsay Cedex, France

Received July 25, 2005

The reaction of $[M(H_2L^i)]$ (M = Cu, Zn) and $U(acac)_4$ in refluxing pyridine produced the trinuclear complexes $[\{ML^i(py)_x\}_2U]$ [L^i = *N,N′*-bis(3-hydroxysalicylidene-R, R = 1,2-ethanediamine (i = 1), 2-methyl-1,2-propanediamine (i = 2), 1,2-cyclohexanediamine (i = 3), 1,2-phenylenediamine (i = 4), 4,5-dimethyl-1,2-phenylenediamine (i = 5), 1,3-propanediamine (i = 6), 2,2-dimethyl-1,3-propanediamine (i = 7), 2-amino-benzylamine (i = 8), or 1,4-butanediamine (i = 9); x = 0 or 1]. The crystal structures show that the central U^{IV} ion adopts the same dodecahedral configuration in all of these compounds, while the Cu^{II} ion coordination geometry and the Cu···U distance vary with the length of the diimino chain of the Schiff base ligand L^i. These geometrical parameters have a major influence on the magnetic properties of the complexes. For the smallest Cu···U distances (i = 1–5), the Cu–U coupling is antiferromagnetic and weak antiferromagnetic interactions are present between the Cu^{II} ions, while for the largest Cu···U distances (i = 6–9), the Cu–U coupling is ferromagnetic and no interaction is observed between the Cu^{II} ions. The magnetic behavior of the $[\{CuL^i\}_2Th]$ compounds (i = 1, 2), in which the Th^{IV} ion is diamagnetic, confirms the presence of weak intramolecular antiferromagnetic coupling between the Cu^{II} ions.

Introduction

Since the discovery, in 1985, of a ferromagnetic interaction in Cu_2Gd complexes,[1] the exchange coupling between a 4f ion and a spin carrier, 3d ion or organic radical, has been studied for both its fundamental aspects, with the aim to elaborate an accurate theoretical model of the interaction, and its applications, especially in the building of molecule-based magnets.[2] Recently, compounds with high nuclearity including clusters,[3] 1D chains,[4] and 2D[5] and 3D[6] polymers have attracted much attention; among these, single-molecule magnets[7] and the first single-chain magnet[8] were characterized. Most of the studies of 3d−4f compounds have been and are still devoted to systems containing isotropic gadolinium(III) as the lanthanide counterpart.[9] Although the interaction between Gd^{III} and a series of spin carriers is ferromagnetic in most cases, in agreement with the theoretical

* To whom correspondence should be addressed. E-mail: salmon@drecam.cea.fr (L.S.); ephri@drecam.cea.fr (M.E.).

† CEA/Saclay.

‡ CNRS-Université de Paris-Sud.

(1) Bencini, A.; Benelli, C.; Caneschi, A.; Carlin, L.; Dei, A.; Gatteschi, D. *J. Am. Chem. Soc.* **1985**, *107*, 8128.

(2) (a) Winpenny, R. E. P. *Chem. Soc. Rev.* **1998**, *27*, 447. (b) Sakamoto, M.; Manseki, K.; Okawa, H. *Coord. Chem. Rev.* **2001**, *219*, 379. (c) Benelli, C.; Gatteschi, D. *Chem. Rev.* **2002**, *102*, 2369.

(3) (a) Tang, J. K.; Wang, Q. L.; Si, S. F.; Liao, D. Z.; Jiang, Z. H.; Yan, S. P.; Cheng. P. *Inorg. Chim. Acta* **2005**, *358*, 325. (b) Sun, Y. Q.; Liang, M.; Dong, W.; Yang, G. M.; Liao, D. Z.; Jiang, Z. H.; Yan, S. P.; Cheng, P. *Eur. J. Inorg. Chem.* **2004**, 1514. (c) Yang, Y. Y.; Huang, Z. Q.; He, F.; Chen, X. M.; Ng, S. W. *Z. Anorg. Allg. Chem.* **2004**, *630*, 286. (d) Zou, Y.; Liu, W. L.; Gao, S.; Lu, C. S.; Dang, D. B.; Meng, Q. J. *Polyhedron* **2004**, *23*, 2253. (e) Zhang, J. J.; Sheng, T. L.; Xia, S. Q.; Leibeling, G.; Meyer, F.; Hu, S. M.; Fu, R. B.; Xiang, S. C.; Wu, X. T. *Inorg. Chem.* **2004**, *43*, 5472.

(4) (a) Koner, R.; Drew, M. G. B.; Figuerola, A.; Diaz, C.; Mohanta, S. *Inorg. Chim. Acta* **2005**, *358*, 3041. (b) Novitchi, G.; Costes, J. P.; Donnadieu, B. *Eur. J. Inorg. Chem.* **2004**, 1808. (c) Costes, J. P.; Novitchi, G.; Shova, S.; Dahan, F.; Donnadieu, B.; Tuchagues, J. P. *Inorg. Chem.* **2004**, *43*, 7792. (d) Gheorghe, R.; Andruh, M.; Costes, J. P.; Donnadieu, B. *Chem. Commun.* **2003**, 2778. (e) Kou, H. Z.; Zhou, B. C.; Wang, R. J. *Inorg. Chem.* **2003**, *42*, 7658. (f) Figuerola, A.; Diaz, C.; Ribas, J.; Tangoulis, V.; Sangregorio, C.; Gatteschi, D.; Maestro, M.; Mahia, J. *Inorg. Chem.* **2003**, *42*, 5274. (g) He, Z.; He, C.; Gao, E. Q.; Wang, Z. M.; Yang, X. F.; Liao, C. S.; Yan, C. H. *Inorg. Chem.* **2003**, *42*, 2206.

(5) (a) Wu, A. Q.; Guo, G. H.; Yang, C.; Zheng, F. K.; Liu, X.; Guo, G. C.; Huang, J. S.; Dong, Z. C.; Takano, Y. *Eur. J. Inorg. Chem.* **2005**, 1947. (b) He, F.; Tong, M. L.; Yu, X. L.; Chen, X. M. *Inorg. Chem.* **2005**, *44*, 559. (c) Zhang, J. J.; Xia, S. Q.; Sheng, T. L.; Hu, S. M.; Leibeling, G.; Meyer, F.; Wu, X. T.; Xiang, S. C.; Fu, R. B. *Chem. Commun.* **2004**, 1186. (d) Kou, H. Z.; Zhou, B. C.; Gao, S.; Wang. R. J. *Angew. Chem., Int. Ed.* **2003**, *42*, 3288.

10.1021/ic0512375 CCC: $33.50
Published on Web 12/07/2005

arguments first proposed,[10,11] the ferromagnetic behavior is not intrinsic since it was found later that the sign of the interaction, ferro- or antiferromagnetic, depends on the nature of the ligands around the metal ions, the donor strength of the organic radical, and the structural parameters.[12−18] The 3d−4f or organic radical−4f interaction is even more complicated when the lanthanide(III) ion is not gadolinium and has an orbital contribution because the magnetic properties are then governed by both the thermal population of the Stark components of the 4f ion and the exchange coupling. The empirical approach that has been developed to determine the nature of the exchange interaction in such systems consists of subtracting the temperature-dependent contribution from the thermal population of the excited levels of the ground *J* multiplet of the 4f ion from the magnetic properties of the exchange-coupled complex; this temperature-dependent contribution is determined from the magnetic behavior of an isostructural compound in which the lanthanide ion is present in a diamagnetic environment.[19,20] From the theoretical model advanced by Kahn et al., the coupling of $4f^n$ ions with other paramagnetic species is expected to be antiferromagnetic for $n < 7$ and ferromagnetic for $n > 7$.[11,20] However, deviations from these predictions were observed in a few series of spin carrier−4f molecular compounds which have been studied up to now;[19−21] here again, it was pointed out that the magnetic properties can be much influenced by small changes induced by ligand field.

In recent years, the first molecular compounds exhibiting a magnetic coupling between 3d and 5f ions have been isolated.[22,23] The magnetic behavior of the trinuclear complexes $[\{CuL^i(py)_x\}_2U]$ in which the central U^{IV} ion is associated with the two Cu^{II} ions by means of a hexadentate Schiff base ligand [H_4L^i = *N*,*N*′-bis(3-hydroxysalicylidene)-R] appeared to depend on the nature of the diimino chain R; the Cu−U interaction was found to be antiferromagnetic for R = 2-methyl-1,2-propanediamine ($i = 2$) and ferromagnetic for R = 1,3-propanediamine ($i = 6$) and dimethyl-1,3-propanediamine ($i = 7$).[23] These results revealed that the Cu−U interaction, like the 3d−4f and organic radical−4f interactions, is very sensitive to slight variations in the structure of the complexes. The most significant structural features to which the sign of the Cu−U coupling could be related concerned the Cu^{II} ion coordination and the Cu···U separation. To check the validity of this assumption, a comparative study of the structures and magnetic properties of a series of new trinuclear complexes of the general formula $[\{ML^i(py)_x\}_2U]$ (M = Cu, Zn) was necessary. Here, we present this analysis for the compounds in which the Lewis base ligands L^i, represented in Scheme 1, differ in the length of their diimino chain (1,2-ethanediamine, $i = 1$; 1,2-cyclohexanediamine, $i = 3$; 1,2-phenylenediamine, $i = 4$; 4,5-dimethyl-1,2-phenylenediamine, $i = 5$; 2-aminobenzylamine, $i = 8$; and 1,4-butanediamine, $i = 9$); we also describe the magnetic behavior of the thorium derivatives $[\{CuL^i\}_2Th]$ ($i = 1, 2$) which permitted the measurement of the weak intramolecular coupling between the Cu^{II} ions in these compounds.

Experimental Section

All reactions were carried out under argon (<5 ppm oxygen or water) using standard Schlenk-vessel and vacuum-line techniques or in a glovebox. Solvents were dried by standard methods and distilled immediately before use; deuterated pyridine (Eurisotop) was distilled over NaH and stored over 3 Å molecular sieves. The ^{1}H NMR spectra were recorded on a Bruker DPX 200 instrument and referenced internally using the residual protio solvent resonances relative to tetramethylsilane (δ 0). Magnetic susceptibility data were recorded on a MPMS5 magnetometer (Quantum Design). The powdered and desolvated samples of the compounds were introduced in capsules in a glovebox and kept under an inert

(6) (a) Yue, Q.; Yang, J.; Li, G. H.; Li, G. D.; Xu, W.; Chen, J. S.; Wang, S. N. *Inorg. Chem.* **2005**, *44*, 5241. (b) An, H.; Xiao, D.; Wang, E.; Li, Y.; Wang, X.; Xu, L. *Eur. J. Inorg. Chem.* **2005**, 854. (c) Cai, Y. P.; Su, C. Y.; Li, G. B.; Mao, Z. W.; Zhang, C.; Xu, A. W.; Kang, B. S. *Inorg. Chim. Acta* **2005**, *358*, 1298. (d) Zhang, J. J.; Sheng, T. L.; Hu, S. M.; Xia, S. Q.; Leibeling, G.; Meyer, F.; Fu, Z. Y.; Chen, L.; Fu, R. B.; Wu, X. T. *Chem.—Eur. J.* **2004**, *10*, 3963.

(7) (a) Mishra, A.; Wernsdorfer, W.; Parsons, S.; Christou, G.; Brechin, E. K. *Chem. Commun.* **2005**, 2086. (b) Mishra, A.; Wernsdorfer, W.; Abboud, K. A.; Christou, G. *J. Am. Chem. Soc.* **2004**, *126*, 15648. (c) Osa, S.; Kido, T.; Matsumoto, N.; Re, N.; Pochaba, A.; Mrozinski, J. *J. Am. Chem. Soc.* **2004**, *126*, 420. (d) Zaleski, C. M.; Depperman, E. C.; Kampf, J. W.; Kirk, M. L.; Pecoraro, V. L. *Angew. Chem., Int. Ed.* **2004**, *43*, 3912.

(8) Costes, J. P.; Clemente-Juan, J. M.; Dahan, F.; Milon, J. *Inorg. Chem.* **2004**, *43*, 8200.

(9) (a) Akine, S.; Matsumoto, T.; Taniguchi, T.; Nabeshima, T. *Inorg. Chem.* **2005**, *44*, 3270. (b) Yamaguchi, T.; Sunatsuki, Y.; Kojima, M.; Akashi, H.; Tsuchimoto, M.; Re, N.; Osa, S.; Matsumoto, N. *Chem. Commun.* **2004**, 1048. (c) Margeat, O.; Lacroix, P. G.; Costes, J. P.; Donnadieu, B.; Lepetit, C. *Inorg. Chem.* **2004**, *43*, 4743. (d) Novitchi, G.; Costes, J. P.; Tuchagues, J. P. *Dalton Trans.* **2004**, 1739. (e) Costes, J. P.; Dahan, F.; Novitchi, G.; Arion, V.; Shova, S.; Lipkowski, J. *Eur. J. Inorg. Chem.* **2004**, 1530.

(10) Benelli, C.; Caneschi, A.; Gatteschi, D.; Guillou, O.; Pardi, L. *Inorg. Chem.* **1990**, *29*, 1750.

(11) Andruh, M.; Ramade, I.; Codjovi, E.; Guillou, O.; Kahn, O.; Trombe, J. C. *J. Am. Chem. Soc.* **1993**, *115*, 1822.

(12) Costes, J. P.; Dahan, F.; Dupuis, A. *Inorg. Chem.* **2000**, *39*, 165. (b) Costes, J. P.; Dahan, F.; Dupuis, A. *Inorg. Chem.* **2000**, *39*, 5994.

(13) Caneschi, A.; Dei, A.; Gatteschi, D.; Sorace, L.; Vostrikova, K. *Angew. Chem., Int. Ed.* **2000**, *39*, 246.

(14) Lescop, C.; Belorizky, E.; Luneau, D.; Rey, P. *Inorg. Chem.* **2002**, *41*, 3375.

(15) Lescop, C.; Luneau, D.; Rey, P.; Bussiere, G.; Reber, C. *Inorg. Chem.* **2002**, *41*, 5566.

(16) Lescop, C.; Bussiere, G.; Beaulac, R.; Belisle, H.; Belorizky, E.; Rey, P.; Reber, C.; Luneau, D. *J. Phys. Chem. Solids* **2004**, *65*, 773.

(17) Caneschi, A.; Dei, A.; Gatteschi, D.; Poussereau, S.; Sorace, L. *Dalton Trans.* **2004**, 1048.

(18) (a) Tsukuda, T.; Suzuki, T.; Kaizaki, S. *Inorg. Chim. Acta* **2005**, *358*, 1253. (b) Tsukuda, T.; Suzuki, T.; Kaizaki, S. *J. Chem. Soc., Dalton Trans.* **2002**, 1721.

(19) Costes, J. P.; Dahan, F.; Dupuis, A.; Laurent, J. P. *Chem.—Eur. J.* **1998**, *4*, 1616.

(20) Kahn, M. L.; Mathonière, C.; Kahn, O. *Inorg. Chem.* **1999**, *38*, 3692.

(21) (a) Kerbellec, N.; Mahé, N.; Guillou, O.; Daiguebonne, C.; Cador, O.; Roisnel, T.; Oushoorn, R. L. *Inorg. Chim. Acta* **2005**, *358*, 3246. (b) Caneschi, A.; Sorace, L.; Casellato, U.; Tomasin, P.; Vigato, P. A. *Eur. J. Inorg. Chem.* **2004**, 3887. (c) Kido, T.; Ikuta, Y.; Sunatsuki, Y.; Ogawa, Y.; Matsumoto, N. *Inorg. Chem.* **2003**, *42*, 398. (d) Figuerola, A.; Diaz, C.; Ribas, J.; Tangoulis, V.; Granell, J.; Lloret, F.; Mahia, J.; Maestro, M. *Inorg. Chem.* **2003**, *42*, 641. (e) Baggio, R.; Garland, M. T.; Moreno, Y.; Pena, O.; Perec, M.; Spodine, E. *J. Chem. Soc., Dalton Trans.* **2000**, 2061.

(22) (a) Le Borgne, T.; Rivière, E.; Marrot, J.; Girerd, J. J.; Ephritikhine, M. *Angew. Chem., Int. Ed.* **2000**, *39*, 1647. (b) Le Borgne, T.; Rivière, E.; Marrot, J.; Thuéry, P.; Girerd, J. J.; Ephritikhine, M. *Chem.—Eur. J.* **2002**, *8*, 774.

(23) (a) Salmon, L.; Thuéry, P.; Rivière, E.; Girerd, J. J.; Ephritikhine, M. *Chem. Commun.* **2003**, 762. (b) Salmon, L.; Thuéry, P.; Rivière, E.; Girerd, J. J.; Ephritikhine, M. *Dalton Trans.* **2003**, 2872.

Scheme 1. Schiff Bases H_4L^i with Their Color Code

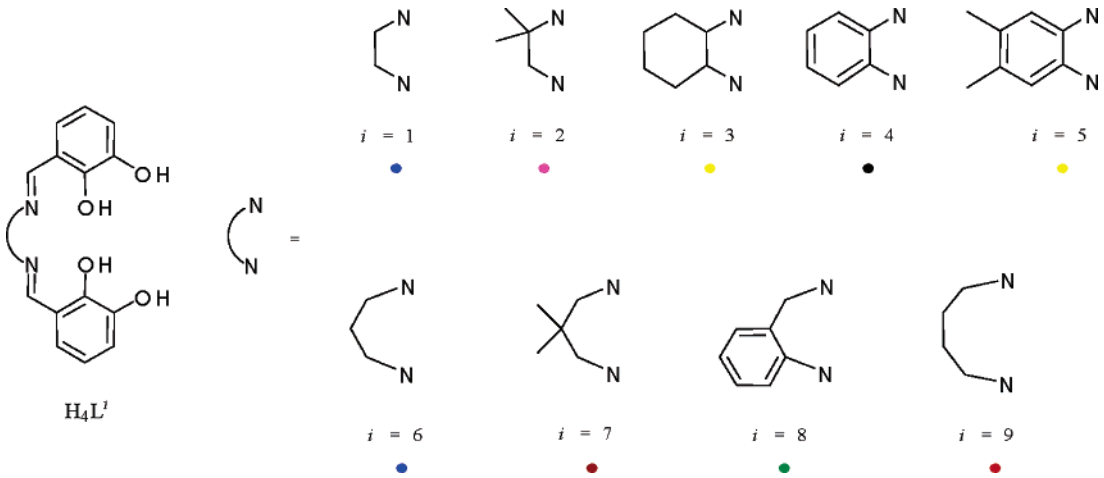

Table 1. Characterization of the Complexes

compound	color yield	analyses[a] C	H	N	NMR spectra[b] salicylidene fragment	diimino chain
$[CuL^1(py)UCuL^1]$	green	50.86	3.14	6.73	*c*	
	84%	(51.14)	(3.31)	(6.63)		
$[\{ZnL^1(py)\}_2U]$	orange	44.89	3.12	7.49	*c*	
	75%	(45.05)	(3.04)	(7.51)		
$[\{CuL^3(py)\}_2U]$	green	48.79	3.62	6.97	5.03, 16.76, 46.15 (3 × 4H, Ph)[d]	−13.62, −11.31, −7.27, −4.02
	57%	(49.06)	(3.76)	(6.87)		(4 × 4H, Cy)[e]
$[\{ZnL^3(py)\}_2U]$	brown	48.83	3.87	7.01	0.72 (4H, CH═N)	−6.41 (4H, NCH)
	41%	(48.91)	(3.75)	(6.85)	3.70, 14.23, 23.87 (3 × 4H, Ph)	−4.53, −3.55, −2.33, −2.18 (4 × 4H, Cy)
$[CuL^4(py)UCuL^4]$	brown	47.52	2.47	6.09	*c*	
	91%	(47.70)	(2.56)	(6.18)		
$[\{ZnL^4(py)\}_2U]$	red	49.63	2.99	7.14	*c*	
	88%	(49.39)	(2.80)	(6.91)		
$[\{CuL^5(py)\}_2U]$	orange	50.86	3.14	6.73	*c*	
	77%	(51.14)	(3.31)	(6.63)		
$[\{ZnL^5(py)\}_2U]$	brown	50.89	3.41	6.78	*c*	
	78%	(50.99)	(3.31)	(6.61)		
$[\{CuL^8(py)\}_2U]$	brown	50.74	3.37	7.47	4.76, 4.91, 16.03, 16.27, 47.08,	−16.79, −5.31, 1.95, 13.10 (4 × 2H, Ph)[e]
	32%	(50.36)	(3.07)	(6.78)	49.01 (6 × 2H, Ph) 433,	
					459 (2 × 2H, $w_{1/2}$ = 2200 Hz, CH═N)	
$[\{ZnL^8(py)\}_2U]$	brown	49.99	3.18	6.90	3.20, 3.34, 5.30, 5.39, 14.32,	−7.40 (4H, NCH_2)
	43%	(50.21)	(3.06)	(6.75)	14.38, 23.79, 24.46 (8 × 2H, Ph and CH═N)	−0.07, 0.55, 1.21, 1.38 (4 × 2H, Ph)
$[\{CuL^9(py)\}_2U]$	red	46.95	3.68	7.30	4.62, 15.92, 47.98 (3 × 4H, Ph)[d]	−8.51 (8H, CH_2)
	67%	(47.14)	(3.58)	(7.17)		69.2 (8H, $w_{1/2}$ = 440 Hz, NCH_2)
$[\{ZnL^9(py)\}_2U]$	orange	46.69	3.49	7.34	0.87, 5.44, 13.06,	−8.15, −7.25 (2 × 8H, CH_2 and NCH_2)
	42%	(46.99)	(3.57)	(7.15)	24.28 (4 × 4H, Ph and CH═N)	

[a] Found (calcd). [b] In pyridine-d_5 at 23 °C. [c] Not soluble in organic solvents. [d] The CH═N signal was not visible. [e] The NCH or NCH_2 signal was not visible.

atmosphere before being placed into the magnetometer. The calibration was made at 298 K using a palladium reference supplied by Quantum Design. The independence of the susceptibility value with regard to the applied field was checked at room temperature. The $\chi_M T$ data were collected over a range of 2−300 K at magnetic fields of 1 and 10 KOe and were corrected for diamagnetism. Elemental analyses were performed by Analytische Laboratorien at Lindlar (Germany).

The H_4L^i Schiff bases were synthesized by published methods.[24] The acac compounds $Cu(acac)_2$ and $Zn(acac)_2$ (Aldrich) were used without purification; $U(acac)_4$ and $Th(acac)_4$ were prepared as previously reported.[25] The $[M(H_2L^i)]$ (M = Cu, Zn) complexes were synthesized in THF by the reaction of H_4L^i with 1 mol equiv of $M(acac)_2$.

(24) Aguiari, A.; Bullita, E.; Casellato, U.; Guerriero, P.; Tamburini, S.; Vigato, P. A. *Inorg. Chim. Acta* **1992**, *202*, 157.

Synthesis of the Trinuclear Compounds $[\{ML^i(py)_x\}_2U]$ (M = Cu, Zn). The complexes were prepared using a procedure similar to that used for $[\{CuL^9(py)\}_2U]$. Yields and characterizing data for the entire set of complexes are given in Table 1.

$[\{CuL^9(py)\}_2U]$. A flask was charged with $[Cu(H_2L^9)]$ (150 mg, 0.38 mmol) and $U(acac)_4$ (122 mg, 0.19 mmol) in pyridine (25 mL). The reaction mixture was heated for 48 h at 110 °C; the brown powder of the Cu_2U complex was filtered off, washed with pyridine (20 mL), and dried under vacuum.

$[\{CuL^1\}_2Th]$. An NMR tube was charged with $[Cu(H_2L^1)]$ (24.0 mg, 0.066 mmol) and $Th(acac)_4$ (21.0 mg, 0.033 mmol) in pyridine (0.4 mL). After 24 h at 110 °C, the solution was decanted, and the green powder was washed with pyridine (0.4 mL) and dried under vacuum. Yield: 95% (30.0 mg). Anal. Calcd. for $C_{32}H_{24}N_4O_8Cu_2Th$: C, 40.38; H, 2.52; N, 5.89. Found: C, 40.14; H, 2.36; N, 6.04. No signal was visible on the ^1H NMR spectrum.

[{CuL^2}$_2$Th]. An NMR tube was charged with [Cu(H$_2$L^2)] (8.0 mg, 0.020 mmol) and Th(acac)$_4$ (6.5 mg, 0.010 mmol) in pyridine (0.4 mL). After 24 h at 110 °C, dark red crystals of [{CuL^2}$_2$Th]·1.5py suitable for X-ray diffraction analysis were deposited.

Crystallographic Data Collection and Structure Determination. The data were collected at 100(2) K on a Nonius Kappa-CCD area detector diffractometer[26] using graphite-monochromated Mo Kα radiation (λ = 0.71073 Å). The crystals were introduced in glass capillaries with a protective "Paratone-N" oil (Hampton Research) coating. The unit cell parameters were determined from 10 frames, and then they were refined on all data. The data (φ scans with 2° steps) were processed with HKL2000.[27] The structures were solved by direct methods or Patterson map interpretation with SHELXS-97 and subsequent Fourier-difference synthesis and refined by full-matrix least-squares on F^2 with SHELXL-97.[28] Absorption effects were corrected empirically with the DELABS program in PLATON.[29] In all compounds, all non-hydrogen atoms were refined with anisotropic displacement parameters, except when mentioned below. The hydrogen atoms were introduced at calculated positions (except in the disordered parts when present) and were treated as riding atoms with a displacement parameter equal to 1.2 (CH, CH$_2$) or 1.5 (CH$_3$) times that of the parent atom. Specific details are as follows.

In [{ZnL^1(py)}$_2$U]·2.5py, the pyridine molecule bound to atom Zn(2) is disordered over two positions which were refined with occupancy parameters constrained to sum to unity and with restraints on bond lengths and displacement parameters. One solvent pyridine molecule is disordered around a symmetry center and has been refined as an idealized hexagon with a common isotropic displacement parameter for all the atoms.

In [{ZnL^8(py)}$_2$U]·1.5py, the bridge connecting N(3) and N(4) is disordered over two positions which were refined with occupancy parameters constrained to sum to unity. Two pyridine solvent molecules were affected with occupancy factors of 0.5, the first to keep acceptable displacement parameters and the second to account for the incompatibility of its location with one of the disordered positions of the bridge. The third solvent molecule is disordered around a symmetry center. The aromatic rings in the disordered parts, the pyridine ring bound to Zn(2), and the solvent pyridine molecules have been refined as idealized hexagons with some restraints on the displacement parameters. The disordered atoms of the bridge were refined with isotropic displacement parameters.

The unit cell for [{CuL^2}$_2$Th]·1.5py has a β angle very close to 90°, but the orthorhombic system can be rejected on the basis of an analysis of equivalent reflections. The structure is isomorphous to those of [{CuL^2}$_2$U]·1.5py and [{NiL^2}$_2$U]·1.5py.[23] The bridge containing C(26) and C(27) and its two methyl substituents is much disordered, but with two (or more) positions being very badly resolved, only the main component has been kept and refined with restraints on bond lengths, angles, and displacement parameters. The pyridine solvent molecules were refined as idealized hexagons with some restraints on the displacement parameters. One of them was affected with an occupancy factor of 0.5 to maintain acceptable displacement parameters. A void in the lattice likely indicates the presence of another, unresolved solvent molecule. The highest residual electron density peak is located near the badly resolved Schiff base bridge.

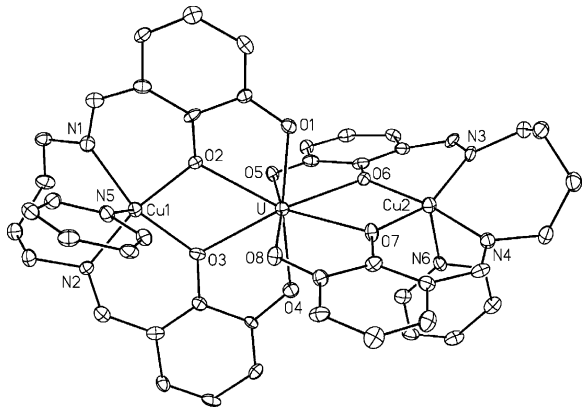

Figure 1. View of the complex [{CuL^9(py)}$_2$U]. The hydrogen atoms are omitted for clarity. The displacement ellipsoids are drawn at the 30% probability level.

A second form of complex [{ZnL^5(py)}$_2$U], likely with two solvent pyridine molecules, has also been obtained, but because it is essentially identical to the first form, it will not be further described herein (see Supplementary Information).

Crystal data and structure refinement details are given in Table 2. The molecular plots were drawn with SHELXTL.[30]

Results and Discussion

Syntheses and Characterization. Treatment of [M(H$_2$L^i)] (M = Cu, Zn) with 0.5 mol equiv of U(acac)$_4$ (acac = MeCOCHCOMe) in refluxing pyridine yielded the trinuclear [{ML^i(py)$_x$}$_2$U] compounds, according to eq 1. The synthesis of the complexes with i = 2, 6, and 7 were previously reported;[22,23] those of the new derivatives are summarized in Table 1.

$$2[M(H_2L^i)] + U(acac)_4 \xrightarrow{\text{pyridine}} [\{ML^i(py)_x\}_2U] + 4acacH \quad (1)$$

Crystals of [{ML^i(py)}$_2$U]·$n$py were obtained from pyridine for M = Cu and i = 9 and for M = Zn and i = 1, 4, 5, 8, and 9. Views of [{CuL^9(py)}$_2$U] and [{ZnL^4(py)}$_2$U] are represented in Figures 1 and 2, respectively. Selected bond lengths and angles are listed in Tables 3 (M = Cu) and 4 (M = Zn), together with those of [{CuL^2}$_2$U], [{CuL^i(py)}U{CuL^i}] (i = 6, 7), and [{ZnL^i(py)}$_2$U] (i = 2, 6, 7) for comparison. Hereafter, these complexes are denoted as [{ML^i}$_2$U], whatever the number of pyridine molecules. All of the trinuclear compounds adopt the same structure with the uranium atom in a dodecahedral environment defined by the oxygen atoms of the Schiff base ligands which form two orthogonal trapezia, O(1)−O(2)−O(3)−O(4) and O(5)−O(6)−O(7)−O(8); the two pairs of oxygen atoms of the salicylidene fragments [O(2), O(3) and O(6), O(7)] are located on the A sites of the trapezia, in the bridging position between the 5f and 3d ions. The latter occupy the inner N$_2$O$_2$ cavities of the bicompartmental Schiff base ligands and are found in a square-pyramidal or square-planar coordination

(25) Vallat, A.; Laviron, E.; Dormond, A. *J. Chem. Soc., Dalton Trans.* **1990**, 921.
(26) *Kappa-CCD Software*; Nonius BV: Delft, The Netherlands, 1998.
(27) Otwinowski, Z.; Minor, W. *Methods Enzymol.* **1997**, *276*, 307.
(28) Sheldrick, G. M. *SHELXS-97* and *SHELXL-97*; University of Göttingen: Göttingen, Germany, 1997.
(29) Spek, A. L. *PLATON*; University of Utrecht: Utrecht, The Netherlands, 2000.
(30) Sheldrick, G. M. *SHELXTL*, version 5.1; University of Göttingen: Göttingen, Germany, 1999, distributed by Bruker AXS, Madison, WI.

Table 2. Crystal Data and Structure Refinement Details

	[{ZnL^1(py)}$_2$U]·2.5py	[{ZnL^4(py)}$_2$U]·3py	[{ZnL^5(py)}$_2$U]·py	[{ZnL^8(py)}$_2$U]·1.5py
empirical formula	$C_{54.5}H_{46.5}N_{8.5}O_8UZn_2$	$C_{65}H_{49}N_9O_8UZn_2$	$C_{59}H_{47}N_7O_8UZn_2$	$C_{59.5}H_{45.5}N_{7.5}O_8UZn_2$
M (g mol^{-1})	1317.27	1452.90	1350.81	1362.30
cryst syst	monoclinic	monoclinic	monoclinic	triclinic
space group	$P2_1/n$	$P2_1/n$	$P2_1/c$	$P\bar{1}$
a (Å)	13.0220(8)	15.7345(11)	13.5131(7)	13.1908(13)
b (Å)	25.3692(19)	21.006(3)	24.7965(15)	15.3953(14)
c (Å)	15.2238(9)	17.375(2)	16.0543(5)	16.0568(18)
α (deg)	90	90	90	107.043(6)
β (deg)	95.136(4)	105.069(6)	109.326(3)	99.595(6)
γ (deg)	90	90	90	110.775(6)
V (Å^3)	5009.1(6)	5545.3(10)	5076.3(4)	2778.1(5)
Z	4	4	4	2
D_{calcd} (g cm^{-3})	1.747	1.740	1.767	1.629
μ(Mo Kα) (mm^{-1})	4.240	3.840	4.186	3.826
F(000)	2596	2872	2664	1342
reflns collected	33533	37313	34471	18660
indep reflns	9412	10431	9515	9527
obsd reflns [$I > 2\sigma(I)$]	5891	4415	6905	5638
R_{int}	0.073	0.063	0.106	0.097
params refined	681	766	698	697
R1	0.052	0.083	0.045	0.071
wR2	0.111	0.155	0.097	0.184
S	0.983	0.966	1.003	0.965
$\Delta\rho_{min}$ (e Å^{-3})	−1.45	−0.85	−1.08	−1.71
$\Delta\rho_{max}$ (e Å^{-3})	0.97	0.77	0.61	1.32

	[{ZnL^9(py)}$_2$U]·2py	[{CuL^9(py)}$_2$U]	[{CuL^2}$_2$Th]·1.5py
empirical formula	$C_{56}H_{52}N_8O_8UZn_2$	$C_{46}H_{42}Cu_2N_6O_8U$	$C_{43.5}H_{39.5}Cu_2N_{5.5}O_8Th$
M (g mol^{-1})	1333.83	1171.97	1126.43
cryst syst	monoclinic	monoclinic	monoclinic
space group	$P2_1/c$	$P2_1/c$	$P2_1/c$
a (Å)	18.0082(16)	19.7974(11)	10.3309(6)
b (Å)	15.5536(9)	16.0236(10)	13.4676(8)
c (Å)	18.6973(17)	13.0921(8)	31.2129(16)
α (deg)	90	90	90
β (deg)	107.037(3)	91.658(4)	90.019(3)
γ (deg)	90	90	90
V (Å^3)	5007.2(7)	4151.4(4)	4342.7(4)
Z	4	4	4
D_{calcd} (g cm^{-3})	1.769	1.875	1.723
μ(Mo Kα) (mm^{-1})	4.243	4.971	4.444
F(000)	2640	2296	2204
reflns collected	33965	28171	25082
indep reflns	9466	7839	7624
obsd reflns [$I > 2\sigma(I)$]	5592	4525	5710
R_{int}	0.073	0.083	0.068
params refined	676	568	548
R1	0.064	0.047	0.070
wR2	0.121	0.098	0.193
S	0.988	0.966	1.260
$\Delta\rho_{min}$ (e Å^{-3})	−1.04	−1.04	−1.26
$\Delta\rho_{max}$ (e Å^{-3})	0.82	0.99	1.57

mode, depending on whether a pyridine molecule is attached to them or not.

Not surprisingly, the length of the diimino chain of L^i has a marked influence on the coordination of the 3d metal. By passing from L^2 to L^9, the N−Cu−N angles are enlarged by ca. 15°, while the N−Cu−O and O−Cu−O angles are sharpened by ca. 6 and 3° on average, respectively. In all of the [{CuL^i}$_2$U] compounds, the sum of these angles is equal or very close to 360°, indicating that the Cu^{II} ion lies in the plane of the N_2O_2 cavity, even if a pyridine molecule is coordinated to it; as a consequence of the widening of this cavity, the Cu−O and Cu−N distances are lengthened by 0.08 Å on average. However, the inner cavity of L^i does not accommodate so perfectly the larger Zn^{II} ion which is displaced out of the N_2O_2 plane, at a distance varying from 0.65(2) Å for L^4 to 0.34(3) Å for L^9, the sum of the N−Zn−N, N−Zn−O, and O−Zn−O angles increasing from ca. 337 to 354°. For a given L^i, the N−M−N, N−M−O, and O−M−O angles are smaller for M = Zn than for M = Cu, and the variations, by passing from L^1 (identical to L^2, L^4, and L^5) to L^9, are greater for the N−Zn−N angles (ca. 14° for L^6, L^7, and L^8 and 22° for L^9) and smaller for the N−Zn−O and O−Zn−O angles (ca 1° for all ligands), by comparison with those observed for the corresponding angles in the analogous Cu compounds. Concomitantly, the lengthening of the Zn−N and Zn−O distances, by ca. 0.05 Å on average, is smaller than that of the corresponding Cu−N and Cu−O distances.

In contrast, the environment of the uranium atom in the [{ML^i}$_2$U] compounds is affected very little by changing M and L^i; coordination of a pyridine molecule to the 3d ion has no influence either. For a given L^i ligand, the average

Table 3. Selected Bond Lengths (Å) and Angles (deg) in the Cu_2An Complexes (An = U, Th)

	$[\{CuL^2\}_2U]^c$	$[\{CuL^6\}_2U]^{a,c}$	$[\{CuL^7\}_2U]^c$	$[\{CuL^9\}_2U]^d$	$[\{CuL^2\}_2Th]^d$
An−O(1)	2.320(10)	2.319(7), 2.295(8)	2.319(6)	2.316(5)	2.377(12)
An−O(2)	2.395(10)	2.442(6), 2.441(7)	2.434(6)	2.447(5)	2.440(11)
An−O(3)	2.417(10)	2.465(7), 2.440(8)	2.433(6)	2.446(6)	2.458(10)
An−O(4)	2.360(10)	2.301(7), 2.305(8)	2.310(6)	2.284(5)	2.406(10)
An−O(5)	2.325(9)	2.259(7), 2.272(7)	2.312(6)	2.307(6)	2.392(10)
An−O(6)	2.448(10)	2.455(7), 2.463(7)	2.465(6)	2.451(5)	2.465(10)
An−O(7)	2.417(9)	2.466(7), 2.457(7)	2.453(6)	2.445(6)	2.460(10)
An−O(8)	2.311(9)	2.291(7), 2.313(7)	2.274(6)	2.286(6)	2.379(10)
<An−O>	2.37(5)	2.37(9), 2.37(8)	2.38(8)	2.37(8)	2.42(4)
<An−O_b>	2.42(2)	2.46(1), 2.45(1)	2.45(2)	2.447(2)	2.456(9)
<An−O_t>	2.33(2)	2.29(3), 2.30(2)	2.30(2)	2.298(14)	2.389(12)
Cu(1)−O(2)	1.862(11)	1.952(7), 1.955(7)	1.947(6)	1.939(6)	1.889(12)
Cu(1)−O(3)	1.867(12)	1.951(6), 1.957(8)	1.952(6)	1.936(6)	1.865(11)
Cu(1)−N(1)	1.897(14)	1.974(9), 2.000(10)	1.983(8)	2.024(7)	1.869(16)
Cu(1)−N(2)	1.930(15)	2.005(11), 2.001(10)	1.992(7)	1.982(7)	1.963(16)
Cu(1)−N(5)		2.280(10), 2.348(10)	2.293(8)	2.354(7)	
Cu(2)−O(6)	1.858(10)	1.912(7), 1.913(7)	1.925(6)	1.944(6)	1.887(10)
Cu(2)−O(7)	1.870(10)	1.923(7), 1.928(7)	1.912(6)	1.960(6)	1.879(11)
Cu(2)−N(3)	1.933(7)	1.983(7), 1.963(9)	1.976(7)	2.029(7)	1.943(13)
Cu(2)−N(4)	1.942(8)	1.971(9), 1.962(9)	1.970(8)	1.988(7)	1.962(14)
Cu(2)−N(6)				2.431(7)	
<Cu−O>	1.864(5)	1.94(2)	1.93(2)	1.945(11)	1.88(1)
<Cu−N>	1.93(2)	1.98(2)	1.980(9)	2.00(2)	1.93(4)
Cu(1)···An	3.536(2)	3.6478(14), 3.6662(15)	3.634(1)	3.6535(11)	3.574(2)
Cu(2)···An	3.540(2)	3.6709(13), 3.6607(14)	3.648(1)	3.6607(11)	3.576(2)
O(1)−An−O(4)	171.8(4)	169.2(2), 168.4(3)	168.4(2)	168.44(19)	174.5(4)
O(2)−An−O(3)	58.9(4)	59.3(2), 58.7(3)	59.5(2)	58.68(18)	58.8(4)
O(5)−An−O(8)	172.1(3)	169.5(2), 170.4(3)	170.2(2)	167.81(19)	174.9(3)
O(6)−An−O(7)	58.8(3)	57.3(2), 57.8(2)	58.2(2)	59.15(19)	59.0(3)
N(1)−Cu(1)−N(2)	87.8(6)	98.5(4), 98.9(4)	97.3(3)	102.4(3)	88.3(8)
N(3)−Cu(2)−N(4)	88.6(4)	99.3(4), 99.5(4)	98.9(3)	103.2(3)	89.6(4)
N(1)−Cu(1)−O(2)	98.8(5)	91.2(4), 91.1(3)	90.6(3)	89.1(3)	98.3(7)
N(2)−Cu(1)−O(3)	94.6(6)	91.9(4), 91.8(4)	92.9(3)	91.4(3)	93.8(6)
N(3)−Cu(2)−O(6)	97.3(3)	93.5(3), 91.7(4)	91.5(3)	89.7(3)	97.4(4)
N(4)−Cu(2)−O(7)	94.3(3)	91.7(3), 92.3(3)	92.6(3)	90.1(3)	92.9(4)
O(2)−Cu(1)−O(3)	78.7(5)	76.9(3), 75.5(3)	76.6(2)	76.5(2)	79.7(5)
O(6)−Cu(2)−O(7)	79.7(4)	75.9(3), 76.5(3)	77.1(2)	76.5(2)	80.1(4)
Cu(1)−O(2)−An	111.7(5)	111.7(3), 112.6(3)	111.6(3)	112.3(2)	110.7(5)
Cu(1)−O(3)−An	110.6(5)	110.8(3), 112.5(4)	111.4(3)	112.4(2)	110.8(5)
Cu(2)−O(6)−An	109.8(4)	113.8(3), 112.9(3)	111.8(3)	112.3(3)	109.8(4)
Cu(2)−O(7)−An	110.7(4)	112.9(3), 112.6(3)	112.8(3)	111.9(3)	110.3(4)
Cu(1)−An−Cu(2)	173.62(5)	175.92(3), 174.98(4)	177.27(3)	178.51(3)	173.18(6)
α_1[b]	0.6(6)	9.9(2), 7.6(5)	8.5(2)	2.2(5)	0.0(6)
α_2[b]	9.2(5)	1.8(4), 3.6(4)	1.7(3)	3.3(5)	8.2(6)

[a] Values for the two independent molecules. [b] α_1 and α_2 are the dihedral angles between the O_bAnO_b and O_bCuO_b planes. [c] Ref 23. [d] This work.

U−O_b (bridging) and U−O_t (terminal) distances in the Cu_2U complex are longer and shorter, respectively, than those in the Zn_2U analogue, by ca. 0.01 Å; the O_b−U−O_b and O_t−U−O_t angles for M = Cu are smaller and larger, respectively, than those for M = Zn, with a maximum deviation of 3−4°. The uranium atom adopting the same dodecahedral configuration in the Cu_2U and Zn_2U counterparts is essential for the validation of the empirical diamagnetic substitution method. In the absence of a general theoretical model to describe the magnetic susceptibility of the U^{IV} ion in its ligand field, this empirical approach is the only one which allows the determination of the nature of the Cu−U exchange coupling. In each series of $[\{CuL^i\}_2U]$ and $[\{ZnL^i\}_2U]$ complexes, the average U−O_b and U−O_t distances differ at most by 0.05 Å, and very small differences are observed within the O_b−U−O_b angles (average values ranging from 58.3(9) to 58.9(7)° for the Cu_2U complexes and 59.4(3) to 61.1(7)° for the Zn_2U complexes) and O_t−U−O_t angles (average values ranging from 168(1) to 172.0(2)° for the Cu_2U complexes and 166(1) to 170(1)° for the Zn_2U complexes). Moreover, there is no significant relationship between these variations and the structure of the Schiff base L^i. These data indicate that any change in the

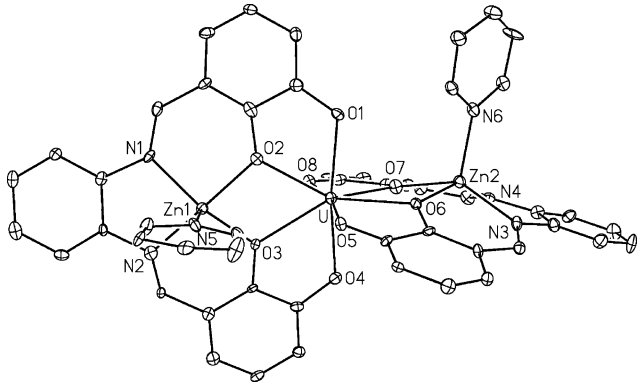

Figure 2. View of the complex $[\{ZnL^4(py)\}_2U]\cdot 3py$. The solvent molecules and hydrogen atoms are omitted for clarity. The displacement ellipsoids are drawn at the 10% probability level.

Table 4. Selected Bond Lengths (Å) and Angles (deg) in the Zn_2U Complexes

	$[\{ZnL^1\}_2U]^b$	$[\{ZnL^2\}_2U]^c$	$[\{ZnL^4\}_2U]^b$	$[\{ZnL^5\}_2U]^b$	$[\{ZnL^6\}_2U]^c$	$[\{ZnL^7\}_2U]^d$	$[\{ZnL^8\}_2U]^b$	$[\{ZnL^9\}_2U]^b$
U−O(1)	2.297(6)	2.372(13)	2.314(9)	2.319(4)	2.315(4)	2.271(9)	2.347(7)	2.292(6)
U−O(2)	2.470(5)	2.400(12)	2.426(10)	2.404(4)	2.418(3)	2.430(8)	2.387(7)	2.416(6)
U−O(3)	2.414(5)	2.404(15)	2.421(8)	2.484(4)	2.426(4)	2.433(10)	2.453(8)	2.452(6)
U−O(4)	2.311(5)	2.392(13)	2.313(10)	2.348(4)	2.306(4)	2.311(10)	2.290(8)	2.310(7)
U−O(5)	2.347(5)	2.324(13)	2.316(8)	2.319(5)	2.317(4)	2.321(10)	2.334(8)	2.294(6)
U−O(6)	2.396(5)	2.402(13)	2.425(8)	2.406(4)	2.427(3)	2.439(9)	2.425(7)	2.464(6)
U−O(7)	2.452(5)	2.425(14)	2.436(9)	2.451(4)	2.432(4)	2.463(12)	2.451(8)	2.436(6)
U−O(8)	2.340(5)	2.332(13)	2.314(9)	2.317(4)	2.304(4)	2.325(8)	2.295(9)	2.341(6)
<U−O>	2.38(6)	2.38(4)	2.37(6)	2.38(6)	2.37(6)	2.37(7)	2.37(6)	2.38(7)
<U−O_b>	2.43(3)	2.41(1)	2.427(6)	2.44(3)	2.426(6)	2.44(1)	2.43(3)	2.44(2)
<U−O_t>	2.32(2)	2.36(3)	2.314(1)	2.326(13)	2.311(6)	2.31(2)	2.32(2)	2.31(2)
Zn(1)−O(2)	2.002(5)	1.985(17)	1.992(9)	1.979(4)	2.044(3)	2.033(9)	2.010(8)	2.018(6)
Zn(1)−O(3)	1.994(5)	2.032(14)	1.977(9)	2.008(4)	2.022(4)	2.040(12)	2.010(8)	2.046(7)
Zn(1)−N(1)	2.015(7)	2.03(2)	2.025(11)	2.059(5)	2.068(5)	2.085(12)	2.053(10)	2.083(8)
Zn(1)−N(2)	2.050(6)	2.12(2)	2.060(12)	2.061(5)	2.071(4)	2.058(12)	2.061(9)	2.081(8)
Zn(1)−N(5)	2.037(6)	2.023(16)	2.042(11)	2.035(6)	2.056(4)	2.114(13)	2.055(6)	2.093(8)
Zn(2)−O(6)	2.003(5)	1.970(12)	1.979(8)	1.982(4)	2.025(4)	2.016(10)	2.015(7)	2.041(6)
Zn(2)−O(7)	1.989(5)	2.021(13)	1.984(9)	1.977(4)	2.020(4)	2.027(11)	2.014(9)	2.050(7)
Zn(2)−N(3)	2.034(6)	2.044(17)	2.058(12)	2.061(5)	2.071(5)	2.122(12)	2.038(13)	2.109(9)
Zn(2)−N(4)	2.025(7)	1.994(16)	2.039(13)	2.039(5)	2.071(6)	2.061(12)	2.034(15)	2.061(8)
Zn(2)−N(6)	2.051(5)	2.077(15)	2.052(13)	2.077(6)	2.090(5)	2.03(2)	2.086(9)	2.081(8)
<Zn−O>	1.997(7)	2.00(3)	1.983(6)	1.987(14)	2.028(11)	2.029(10)	2.012(3)	2.039(12)
<Zn−N>	2.031(15)	2.04(5)	2.046(14)	2.055(11)	2.070(1)	2.08(3)	2.047(13)	2.084(17)
Zn(1)···U	3.6614(9)	3.606(3)	3.6673(17)	3.6473(7)	3.6824(7)	3.718(1)	3.6967(14)	3.7083(12)
Zn(2)···U	3.6631(9)	3.661(2)	3.6542(17)	3.6601(7)	3.6896(7)	3.682(1)	3.7123(15)	3.7248(13)
O(1)−U−O(4)	167.94(18)	170.8(5)	168.8(3)	166.10(15)	165.99(13)	167.0(3)	170.5(3)	167.7(2)
O(2)−U−O(3)	60.75(16)	61.6(6)	59.4(3)	60.48(14)	60.61(12)	60.6(3)	59.2(3)	60.3(2)
O(5)−U−O(8)	170.10(19)	168.7(5)	169.9(3)	171.24(15)	167.56(13)	165.0(4)	168.9(3)	167.9(2)
O(6)−U−O(7)	60.02(17)	60.6(4)	59.9(3)	59.42(16)	60.64(12)	60.8(3)	59.6(3)	60.5(2)
N(1)−Zn(1)−N(2)	82.5(3)	82.2(10)	81.1(5)	80.4(2)	97.76(18)	95.9(5)	93.9(4)	104.2(3)
N(3)−Zn(2)−N(4)	82.2(3)	82.2(7)	82.5(5)	81.9(2)	98.2(2)	97.4(5)	91.4(6)	104.4(3)
N(1)−Zn(1)−O(2)	90.8(2)	91.1(8)	91.8(5)	89.27(19)	87.68(16)	88.6(4)	87.9(4)	88.2(3)
N(2)−Zn(1)−O(3)	89.2(2)	86.4(8)	89.6(4)	89.70(19)	89.36(17)	89.3(4)	89.3(3)	87.2(3)
N(3)−Zn(2)−O(6)	89.0(2)	92.9(6)	91.1(4)	88.7(2)	88.51(18)	88.5(4)	89.7(4)	87.6(3)
N(4)−Zn(2)−O(7)	89.8(2)	88.6(6)	89.9(5)	91.6(2)	88.1(2)	88.2(5)	90.0(4)	88.8(3)
O(2)−Zn(1)−O(3)	76.4(2)	75.5(6)	74.5(4)	76.29(17)	73.92(14)	74.1(4)	73.0(3)	74.0(3)
O(6)−Zn(2)−O(7)	74.8(2)	75.2(5)	75.5(4)	74.91(18)	74.65(14)	75.7(4)	73.9(3)	74.2(3)
Zn(1)−O(2)−U	109.5(2)	110.3(8)	111.9(5)	112.30(19)	110.96(15)	112.5(4)	114.3(3)	113.2(3)
Zn(1)−O(3)−U	112.0(2)	108.5(7)	112.6(4)	108.12(18)	111.46(15)	112.1(5)	111.5(3)	110.8(3)
Zn(2)−O(6)−U	112.5(2)	113.3(5)	111.7(4)	112.7(2)	111.61(15)	111.1(4)	113.2(4)	111.2(3)
Zn(2)−O(7)−U	110.7(2)	110.5(6)	111.2(4)	111.1(2)	111.61(16)	109.8(5)	112.1(4)	112.0(3)
Zn(1)−U−M(2)	172.77(2)	168.59(6)	169.11(4)	165.869(18)	169.172(15)	170.9(3)	175.97(4)	171.09(3)
$\alpha_1{}^a$	10.6(3)	18.3(7)	11.3(5)	14.9(1)	15.4(2)	7.1(3)	12.5(2)	11.5(4)
$\alpha_2{}^a$	12.3(2)	5.4(3)	11.5(2)	12.2(2)	10.7(3)	14.2(3)	9.9(5)	13.1(4)

[a] α_1 and α_2 are the dihedral angles between the O_bUO_b and O_bZnO_b planes. [b] This work. [c] Ref 23. [d] Ref 22.

magnetic behavior of the $[\{CuL^i\}_2U]$ compounds could clearly not be attributable to modifications in the ligand field of the U^{IV} ion.

In the $[\{CuL^i(py)_x\}_2U]$ complexes, the dihedral angles, α, between the O_b-U-O_b and O_b-Cu-O_b planes are small, with average values ranging from 2.8(6) to 6(3)°, and they do not vary with the length of the diimino chain of L^i and the number of coordinated pyridine molecules since in all of these complexes, the Cu^{II} ions are invariably found in the N_2O_2 plane of the orthogonal Schiff base ligands. The most significant geometrical difference between the CuO_2U bridging cores, by changing L^i, is the increase of the Cu···U distance which varies from the average value of 3.538(2) Å for L^2 to 3.657(4) Å for L^9 in relation to the variation in the O_b-Cu-O_b angle (Scheme 2).

The $[\{CuL^i\}_2Th]$ ($i = 1, 2$) complexes have been synthesized by reaction of $[Cu(H_2L^i)]$ and $Th(acac)_4$ in pyridine. The analytically pure green powder of $[\{CuL^1\}_2Th]$ was isolated in a 95% yield; the structure of the dark red crystals of $[\{CuL^2\}_2Th]\cdot 1.5py$, which is isomorphous to that of the uranium analogue, is represented in Figure 3, and selected bond lengths and angles are listed in Table 3. The average $Th-O_b$ and $Th-O_t$ distances, 2.456(9) and 2.389(12) Å, respectively, are larger than the average $U-O_b$ and $U-O_t$ distances in the uranium counterpart (2.42(2) and 2.33(2) Å). These variations reflect the difference in the radii of the Th^{IV} and U^{IV} ions.[31] The geometry of the CuO_2An (An = Th, U) bridging cores and the environment of the Cu^{II}

Scheme 2. Modifications in the Cu^{II} Ion Coordination and the Cu···U Distance in the Complexes $[\{CuL^i\}_2U]$ by Passing from L^{1-5} (red line) to L^{6-9} (black line)

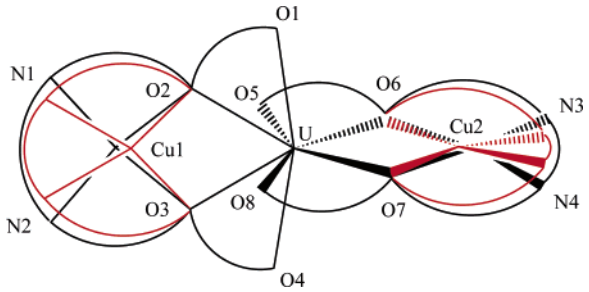

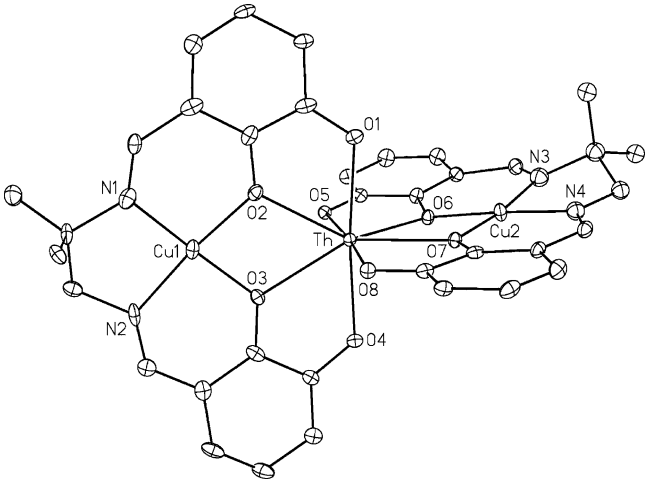

Figure 3. View of the complex [{CuL^2}$_2$Th]·1.5py. The solvent molecules and hydrogen atoms are omitted for clarity. The displacement ellipsoids are drawn at the 10% probability level.

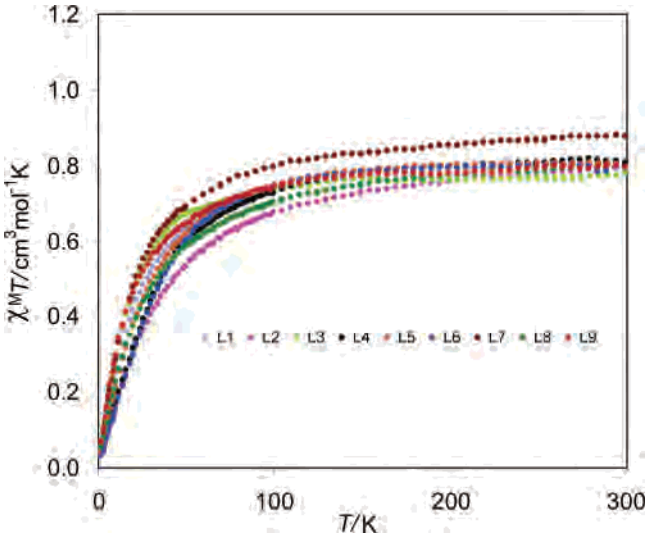

Figure 4. Thermal dependence of $\chi_M T$ for the complexes [{ZnL^i}$_2$U].

ions are quite identical in both compounds. It is also noteworthy that the variations in the corresponding bond distances and angles of the [{CuL^2}$_2$Th] and [{CuL^7}$_2$Th][22b] complexes are identical to those observed in the uranium analogues; in particular, the average Cu···Th distance of 3.69(1) Å in [{CuL^7}$_2$Th] is 0.12 Å larger than that in [{CuL^2}$_2$Th].

The shortest intermetallic Cu···Cu distances between two distinct [{CuL^i}$_2$U] complexes are equal to 5.922(4) (L^2), 6.007(3) (L^6), 6.446(3) (L^7), and 6.6898(6) Å (L^9); the trinuclear entities may thus be considered to be magnetically isolated.

Magnetic Properties. The magnetic behavior of the trinuclear [{ZnL^i}$_2$U] (i = 1−9) complexes is represented in Figure 4 in the form of a $\chi_M T$ versus T plot. For those compounds in which the Zn^{II} ion is diamagnetic, the $\chi_M T$ values at room temperature, roughly 0.8 cm^3 mol^{-1} K, represent the contribution of the sole U^{IV} ion in its crystal field; they decrease with T because of the depopulation of

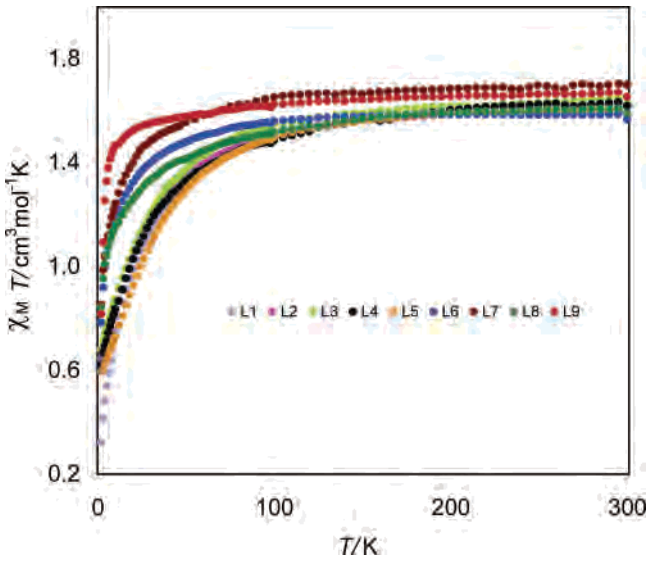

Figure 5. Thermal dependence of $\chi_M T$ for the complexes [{CuL^i}$_2$U].

the Stark sublevels and tend toward being 0 cm^3 mol^{-1} K at 2 K. The room-temperature value is much lower than the theoretical value, 1.6 cm^3 mol^{-1} K, for a 5f^5 free-ion system with a nominal ^{3}H$_4$ ground state.[32a] This decrease is explained by the reduction in symmetry (and the covalency in the bonding) which remove the orbital degeneracies.[32] The value at low temperature is close to but does not reach zero, the expected value for a nonmagnetic singlet ground state for the 5f^2 ion, and indicates that these uranium(IV) systems may have nearly degenerate ground states.[32b] The curves of $\chi_M T$ versus T for these Zn$_2$U compounds are very close, with maximum deviations of 0.15 cm^3 mol^{-1} K at 20 K, in agreement with the fact that the dodecahedral configuration of the uranium atom is quite identical in the trinuclear complexes.

The curves of $\chi_M T$ versus T for the trinuclear [{CuL^i}$_2$U] (i = 1−5) compounds, represented in Figure 5, are almost parallel and deviate by ca. 0.1 cm^3 mol^{-1} K at 10 K. Between 300 and 100 K, the value of $\chi_M T$ is close to 1.6 cm^3 mol^{-1} K and corresponds to that expected for two Cu^{II} and one U^{IV} isolated ions. When the temperature is lowered further, $\chi_M T$ decreases more and more rapidly to reach values between 0.32 and 0.68 cm^3 mol^{-1} K at 2 K (L^1 0.32, L^2 0.64, L^3 0.68, L^4 0.62, and L^5 0.59). These values are smaller than the value, 0.8 cm^3 mol^{-1} K, expected for two noninteracting Cu^{II} ions, and they reflect the presence of an intramolecular antiferromagnetic coupling between these 3d ions. The differences $\Delta(\chi_M T) = (\chi_M T)$[{CuL^i}$_2$U] − $(\chi_M T)$-[{ZnL^i}$_2$U], represented in Figure 6, are equal to approximately 0.8 cm^3 mol^{-1} K between 300 and 100 K, then decrease as T is lowered to reach values ranging from 0.27

(31) Shannon, R. D. *Acta Crystallogr., Sect. A* **1976**, *32*, 751.

(32) (a) Sidall, T. H. In *Theory and Applications of Molecular Paramagnetism*; Boudreaux, E. A., Mulay, L. N., Eds.; John Wiley & Sons: New York, 1976; Chapter 6. (b) Jantunen, K. C.; Batchelor, R. J.; Leznoff, D. B. *Organometallics* **2004**, *23*, 2186. (c) Hirose, M.; Miyake, C. *Inorg. Chim. Acta*, **1988**, *150*, 293. (d) Kanellakopulos, B. In *Organometallics of the f-Elements*; Marks, T. J., Fischer, R. D., Eds.; Nato Advanced Study Institutes Series; D. Reidel: Dordrecht, The Netherlands, 1978. (e) Jantunen, K. C.; Haftbaradaran, F.; Katz, M. J.; Batchelor, R. J.; Schatte, G.; Leznoff, D. B. *Dalton Trans.* **2005**, 3083.

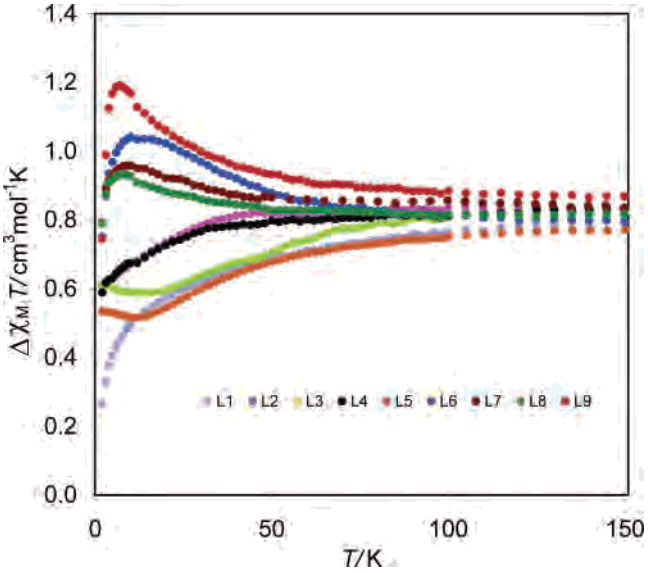

Figure 6. Thermal dependence of $\Delta(\chi_M T) = (\chi_M T)[\{CuL^i\}_2U] - (\chi_M T)[\{ZnL^i\}_2U]$.

to 0.62 $cm^3\ mol^{-1}$ K at 2 K (L^1 0.27, L^2 0.61, L^3 0.62, L^4 0.58, and L^5 0.53). Therefore, the exchange interaction between the Cu^{II} and U^{IV} ions is antiferromagnetic in these $[\{CuL^i\}_2U]$ complexes ($i = 1-5$).

The curves of $\chi_M T$ versus T for the trinuclear $[\{CuL^i\}_2U]$ ($i = 6-9$) compounds are almost parallel and deviate by ca. 0.3 $cm^3\ mol^{-1}$ K at 10 K (Figure 5). Between 300 and 100 K, the value of $\chi_M T$ is close to 1.6 $cm^3\ mol^{-1}$ K, but when the temperature is lowered, the profiles of the plots are different from those previously observed for $i = 1-5$. The $\chi_M T$ products decrease less rapidly and at 2 K, they reach values between 0.85 and 0.78 $cm^3\ mol^{-1}$ K (L^6 0.78, L^7 0.85, L^8 0.85, and L^9 0.82). The differences, $\Delta(\chi_M T) = (\chi_M T)[\{CuL^i\}_2U] - (\chi_M T)[\{ZnL^i\}_2U]$, represented in Figure 6, are equal to approximately 0.8 $cm^3\ mol^{-1}$ K between 300 and 100 K, then increase as T is lowered to reach a maximum value of 0.93−1.1 $cm^3\ mol^{-1}$ K (L^6 1.05, L^7 0.95, L^8 0.93, and L^9 1.19), and finally drop to 0.70−0.79 $cm^3\ mol^{-1}$ K at 2 K (L^6 0.75, L^7 0.79, L^8 0.79, and L^9 0.75). These values are close to that expected for two noninteracting Cu^{II} ions. Therefore, the interaction between the Cu^{II} and U^{IV} ions in these $[\{CuL^i\}_2U]$ ($i = 6-9$) complexes is ferromagnetic.

The field dependence at 2 K of the difference $\Delta M = M[\{CuL^i\}_2U] - M[\{ZnL^i\}_2U]$, where M is the magnetization, is represented in Figure 7. For $i = 6$, 7, and 8, ΔM closely follows the Brillouin function for two noninteracting Cu^{II} ions, which is consistent with the values of $\Delta(\chi_M T)$ at this temperature, 0.75−0.79 $cm^3\ mol^{-1}$ K. However, the curves of ΔM for the complexes $[\{CuL^i\}_2U]$ ($i = 1-5$) reveal the presence of antiferromagnetic interactions between the Cu^{II} ions. The greatest deviation is observed with $[\{CuL^1\}_2U]$ which exhibits the lowest value of $\Delta(\chi_M T)$ at 2 K, 0.27 $cm^3\ mol^{-1}$ K, while the ΔM curves for the other complexes ($i = 2-5$) are similar and correspond to the close values of $\Delta(\chi_M T)$ which range from 0.53 to 0.62 $cm^3\ mol^{-1}$ K. These features confirm the presence of antiferromagnetic interactions between the Cu^{II} ions in the $[\{CuL^i\}_2U]$ complexes with $i = 1-5$.

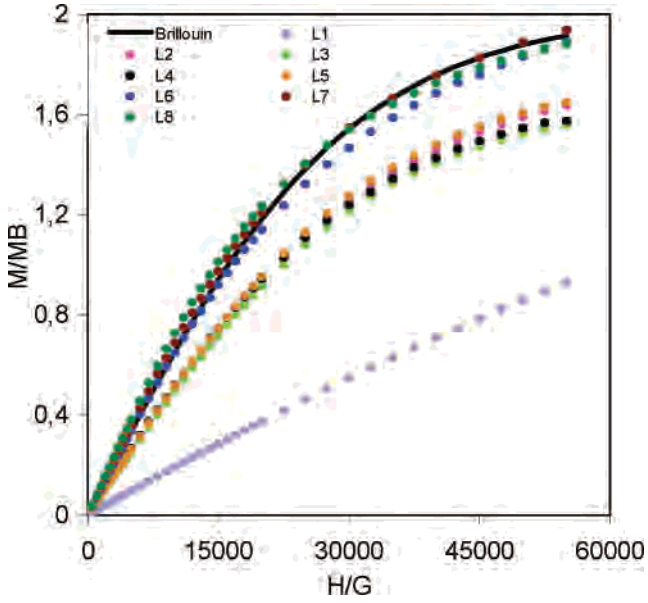

Figure 7. Field dependence of the difference $\Delta M = M[\{CuL^i\}_2U] - M[\{ZnL^i\}_2U]$ at 2 K. The solid line corresponds to the Brillouin function for two non interacting Cu^{II} ions.

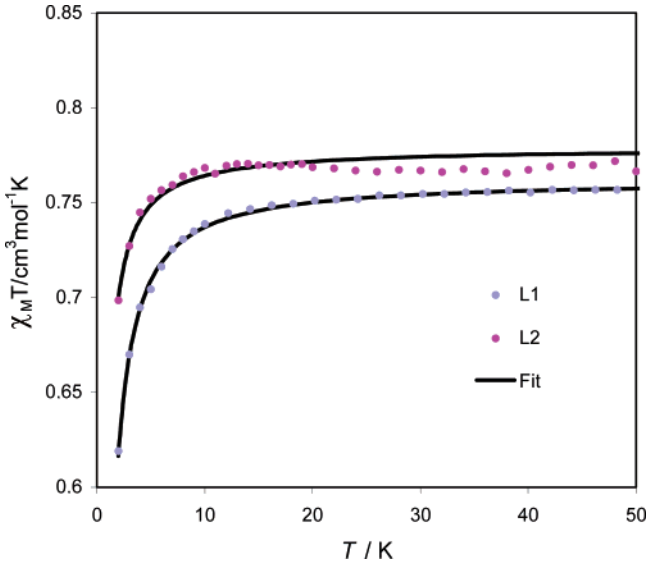

Figure 8. Thermal dependence of $\chi_M T$ for the complexes $[\{CuL^i\}_2Th]$ ($i = 1$, 2). The solid line was generated from the best fit parameters given in the text.

The intramolecular antiferromagnetic couplings between the Cu^{II} ions in the $[\{CuL^i\}_2U]$ complexes ($i = 1$, 2) were further confirmed by the magnetic behavior of the Cu_2Th analogues in which the Th^{IV} ion is diamagnetic; the variation of $\chi_M T$ versus T is represented in Figure 8. The $\chi_M T$ products are equal to 0.75 $cm^3\ mol^{-1}$ K down to 20 K, but then they decrease to reach values of 0.62 and 0.70 $cm^3\ mol^{-1}$ K at 2 K, for $i = 1$ and 2, respectively. In contrast, it was previously reported that for $[\{CuL^7\}_2Th]$, the $\chi_M T$ product is essentially constant and equal to 0.77 $cm^3\ mol^{-1}$ K between 300 and 2 K, showing the absence of any Cu−Cu interaction. The susceptibility data were fitted by using the HDVV isotropic spin Hamiltonian $H = -JS_{Cu1}S_{Cu2}$, with $S_{Cu1} = S_{Cu2} = 1/2$.[33] A very good agreement between the experimental and calculated values is obtained by taking $J_{Cu-Cu} = -0.84\ cm^{-1}$

and $g_{Cu} = 2.016$ for $[\{CuL^1\}_2Th]$ and $J_{Cu-Cu} = -0.48$ cm^{-1} and $g_{Cu} = 2.029$ for $[\{CuL^2\}_2Th]$. It is noteworthy that the J_{Cu-Cu} parameters were found to be negative (and the interaction antiferromagnetic)[12,34] or equal to zero[10,11,35] in a variety of Cu_2Ln complexes (Ln = Gd, La, Lu) with the exception of the recently reported Cu_2Gd compound $[\{LCu)_2Gd(CF_3CO_2)_3]$ [L = *N*,*N*′-bis(salicylidene)-1,3-propanediamine] in which a ferromagnetic coupling between the Cu^{II} ions was shown; this unique behavior was accounted for by the existence of $\pi-\pi$ interactions between the phenyl rings of the ligands.[36]

The comparison of the crystal structures of the $[\{CuL^i\}_2U]$ complexes does not permit correlation of their distinct magnetic properties to any variation in the coordination geometry of the U^{IV} ion which adopts the same dodecahedral configuration. That the nature of L^i has practically no effect on the uranium environment is also shown by the quite similar profiles of the $\chi_M T$ versus T curves for the $[\{ZnL^i\}_2U]$ compounds (Figure 4).

Magnetic studies on polynuclear transition metal complexes, in particular Cu^{II} dimers[37] and $Cu^{II}Ni^{II}$ binuclear species[38] with di-μ-hydroxo or di-μ-phenoxo bridges, demonstrated that the nature and strength of the exchange interaction is influenced by the bending of the bridging network and the distance between the metal centers. However, the differences in the magnetic behavior of the Cu_2U complexes cannot be connected with the dihedral angle between the two halves of the CuO_2U bridging core. The most obvious structural modifications induced by changing the Schiff base ligand L^i concern the Cu^{II} coordination and the Cu···U separation. The distance between the two metallic centers increases by 0.10−0.12 Å when the number of carbon atoms of the diimino chain increases from 2 ($i = 1-5$) to 3 ($i = 6-8$) and 4 ($i = 9$). For the largest Cu···U distances ($i = 6-9$), the Cu−U coupling is ferromagnetic, and no interaction is observed between the Cu^{II} ions, while for the smallest Cu···U distances ($i = 1-5$), the Cu−U coupling is antiferromagnetic, and the overall antiferromagnetism of the trinuclear complexes is enhanced by weak antiferromagnetic interactions between the Cu^{II} ions. For $i = 1$ and 2, the antiferromagnetic coupling between the Cu^{II} ions in the Cu_2U complexes is stronger than that in the Cu_2Th counterparts, as shown by the values of $\chi_M T$ at 2 K (0.27 and 0.62 cm^3 mol^{-1} K, respectively, for $i = 1$); this trend is in line with the Cu···U distance which is ca. 0.04 Å shorter than the Cu···Th distance.

These variations in the magnitude and sign of the Cu−U exchange coupling are reminiscent of those of the 3d−Gd or radical−Gd magnetic interaction. From the magnetic properties of several Cu_nGd_n complexes, it was first proposed that the value of the ferromagnetic J_{Cu-Gd} parameter decreased with the Cu···Gd distance by following an exponential function.[39] Another study of strictly dinuclear CuGd compounds containing a CuO_2Gd bridging core revealed that the ferromagnetic interaction increased with the bending of the core, measured by the dihedral angle, α, between the two halves, O−Cu−O and O−Gd−O, of the bridging part; in these complexes, the values of J_{Cu-Gd} were better correlated with the exponential of the angle α than with the exponential of the Cu···Gd distance.[12] Assuming that the ferromagnetic character of the Cu−Gd interaction is the result of coupling between the 4f−3d ground configuration and the excited configuration resulting from the $3d_{Cu} \rightarrow 5d_{Gd}$ electron transfer, the decrease of the Cu−Gd coupling caused by the bending of the CuO_2Gd bridging core was related to the decrease of the β_{5d-3d} transfer integrals. Even more striking was the discovery of antiferromagnetic 3d−Gd or radical−Gd exchange interactions. In the trinuclear Cu_2Gd complexes with a μ-phenolato-μ-oximato core[12] or the binuclear vanadyl-gadolinium compounds with a VO_2Gd bridging motif,[40] the change of the magnetic behavior from ferromagnetic to antiferromagnetic was, here again, related to the increase in the bending of the bridging core; the emergence of antiferromagnetism was then accounted for by the occurrence of either the Heitler−London interaction[41] or the Anderson mechanism.[42] Recent quantum chemical calculations led to the conclusion that the Cu−Gd interaction is intrinsically ferromagnetic in the large majority of complexes which generally exhibit a pseudo-C_{2v} geometry; exceptions to this rule appear when the molecular asymmetry is advanced because of the strong chemical nonequivalence of the donor atoms.[43] Such symmetry arguments cannot be taken into consideration for explaining the magnetic properties of the $[\{CuL^i\}_2U]$ compounds. The structure of the radical−gadolinium complexes is different from that of the 3d−Gd compounds since the radical ligands are directly bound to the metal center and magnetic exchange is not mediated by ancillary organic fragments. In these compounds, no clear magnetostructural correlation is apparent; the radical−Gd coupling in the [Gd(nitroxide radical)$(CF_3COCHCOCF_3)_3$] complexes seems to become more antiferromagnetic as the radical···Gd distance increases, while the

(33) (a) Borrás-Almenar, J. J.; Clemente-Juan, J. M.; Coronado, E.; Tsukerblat, B. S. *Inorg. Chem.* **1999**, *38*, 6081. (b) Borrás-Almenar, J. J.; Clemente-Juan, J. M.; Coronado, E.; Tsukerblat, B. S. *J. Comput. Chem.* **2001**, *22*, 985.

(34) Shiga, T.; Ohba, M.; Okawa, H. *Inorg. Chem. Commun.* **2003**, *6*, 15.

(35) (a) Shiga, T.; Ohba, M.; Okawa, H. *Inorg. Chem.* **2004**, *43*, 4435. (b) Benelli, C.; Fabretti, A.; Giusti, A. *J. Chem. Soc., Dalton. Trans.* **1993**, 409. (c) Bencini, A.; Benelli, C.; Caneschi, A.; Dei, A.; Gatteschi, D. *Inorg. Chem.* **1986**, *25*, 572.

(36) Novitchi, G.; Shova, S.; Caneschi, A.; Costes, J. P.; Gdaniec, M.; Stanica, N. *Dalton Trans.* **2004**, 1194.

(37) (a) Charlot, M. F.; Kahn, O.; Jeannin, S.; Jeannin, Y. *Inorg. Chem.* **1980**, *19*, 1411. (b) Charlot, M. F.; Jeannin, S.; Jeannin, Y.; Kahn, O.; Lucrece-Abaul, J.; Martin-Frere, J. *Inorg. Chem.* **1979**, *18*, 1675. (c) Crawford, V. H.; Richardson, H. W.; Wasson, J. R.; Hodgson, D. J.; Hatfield, W. E. *Inorg. Chem.* **1976**, *15*, 2107.

(38) Journeaux, Y.; Kahn, O.; Morgenstern-Badarau, I.; Galy, J.; Jaud, J.; Bencini, A.; Gatteschi, D. *J. Am. Chem. Soc.* **1985**, *107*, 6305.

(39) Benelli, C.; Blake, A. J.; Milne, P. E. Y.; Rawson, J. M.; Winpenny, E. P. *Chem.—Eur. J.* **1995**, *1*, 614.

(40) Costes, J. P.; Dahan, F.; Donnadieu, B.; Garcia-Tojal, J.; Laurent, J. P. *Eur. J. Inorg. Chem.* **2001**, 363.

(41) (a) Kahn, O. In *Magneto-Structural Correlations in Exchange Coupled Systems*; Willet, R. D., Gatteschi, D., Kahn, O., Eds.; D. Reidel: Dordreicht, The Netherlands, 1985. (b) Girerd, J. J.; Charlot, M. F.; Kahn, O. *Chem. Phys. Lett.* **1981**, *82*, 534.

(42) (a) Anderson, P. W. *Phys. Rev.* **1956**, *115*, 2. (b) Anderson, P. W. In *Magnetism*; Rado, G. T., Suhl, H., Eds.; Academic Press: New York, 1963; Vol. 1, Chapter 2.

(43) Paulovič, J.; Cimpoesu, F.; Ferbinteanu, M.; Hirao, K. *J. Am. Chem. Soc.* **2004**, *126*, 3321.

opposite trend is observed with the nitrato derivatives [Gd(nitroxide radical)$(NO_3)_3$].[14,15] Qualitative correlations between the magnetic properties and the absorption and emission spectra of these compounds were established.[15] The largest antiferromagnetic interaction of $-11.4\ cm^{-1}$ involving gadolinium and radicals or transition metal ions was discovered by using a semiquinonate radical which is a much stronger ligand than the nitroxide-type radicals. This result reinforced the assumption that the more tightly bound radical would favor the direct overlap of the ligand orbitals with the f orbitals, leading to antiferromagnetism, over the overlap with the s and d orbitals which leads to ferromagnetism.[13] The former would more easily become dominant in the uranium complexes because of the greater spatial extension of the 5f orbitals. Thus, bringing the Cu^{II} and U^{IV} ions closer in the $[\{CuL^i\}_2U]$ complexes could effectively cause the change from ferromagnetic to antiferromagnetic.

Conclusion

The magnetic study of a series of trinuclear complexes $[\{CuL^i\}_2U]$, in which the Schiff base ligands, L^i, differ by the length of their diimino chain, show that the Cu−U exchange interaction is strongly dependent on the distance between the 3d and 5f ions. For the shortest Cu···U separations, this interaction is antiferromagnetic, and the overall antiferromagnetism of the trinuclear complexes is enhanced by weak antiferromagnetic interactions between the Cu^{II} ions, while for the largest Cu···U distances, the Cu−U coupling is ferromagnetic, and no interaction is observed between the Cu^{II} ions. This situation is reminiscent of that encountered with the 3d−4f or radical−4f complexes where the sign and magnitude of the magnetic coupling are very sensitive to slight modifications of the ancillary ligands, the radicals, and the electronic structure of the complexes.

Supporting Information Available: Tables of crystal data, atomic positions and displacement parameters, anisotropic displacement parameters, bond lengths and bond angles in CIF format. This material is available free of charge via the Internet at http://pubs.acs.org.

IC0512375